Fabrication of Nickel Oxide Nanocomposite Layer on a Flexible Polyimide Substrate via Ion Exchange Technique

Shuxiang Mu, Dezhen Wu, Yue Wang, Zhanpeng Wu,* Xiaoping Yang, and Wantai Yang

State Key Laboratory of Chemical Resource Engineering, Beijing University of Chemical Technology, Beijing 100029, China

ABSTRACT Continuous nickel oxide (NiO) nanocomposite layer on flexible polyimide (PI) substrate was prepared via an ion exchange technique. First, nickel(II) poly(amate) layers were formed on both surfaces of PI film through chemical surface modification of PI films in aqueous NaOH solution and then ion exchange in aqueous $NiSO_4$ solution. Subsequently, hydrothermal treatment of the Ni^{2+}-loaded PI films in an aqueous urea solution led to $Ni(OH)_2$ formation in the surface-modified layers. Final thermal annealing in ambient air made $Ni(OH)_2$ decompose to NiO, which diffused and aggregated to give continuous layers on both surfaces of PI film. The composite films were characterized by XRD, XPS, SEM, TEM, TGA, and DSC, respectively. Results from SEM and TEM measuring revealed that the NiO layers consisted of NiO nanoparticles with diameter ranging from 10 to 15 nm. Thermal properties of PI/NiO nanocomposite films were similar to those of host PI. This paper provides an effective methodology for the preparation of polymer/metal oxide nanocomposite films, which hold great promise toward the potential application in the areas of flexible microsensors and devices.

KEYWORDS: ion exchange • nanocomposites • nickel oxide • polyimide • surface modification

INTRODUCTION

Transitional metal oxides are key materials in catalysis, microelectronic, optical, and magnetic applications. Considerable efforts have been, therefore, focused on synthesis and characterization of nanocomposites containing transitional oxide nanoparticles, especially polymer/transitional metal oxide nanocomposites as polymer base offers advantages in weight, flexibility, elasticity, fragility, and deployability with respect to inorganic supports such as glass, metals, and ceramics. Among various polymers, polyimide (PI) is a class of versatile high-performance polymer that continues to gain importance in aerospace and electronics applications (1−4). It has excellent thermal stability, high mechanical strength, good film-forming ability, superior radiation and chemical resistance, good adhesions, and low dielectric constant. Therefore, PI is an attractive matrix for composite materials for various devices in which chemical and thermal stability is required. The fabrication of PI/transitional metal oxide nanocomposites has been attracting increased attention because of the advantages of coupling of the two components.

The polymer/metal oxide composites have been traditionally prepared by mixing metal oxide nanoparticles with polymer solution and followed curing of the material (5, 6) or sputtering metal oxide on polymer substrate (7). However, these processes often lead to inhomogeneous dispersion and uncontrollable size distribution of the metal oxide particles. Another route for preparing PI/metal oxide nanocomposites is the in situ synthesis process which works by dissolving a metal salts or complex within polymeric precursor solution and decomposing to its corresponding metal oxides while curing or drying the films (8−12). The advantage of this process is the uniform distribution of the metal oxide source (typically metal ions) and the structure homogeneity of the precursors, which provides a resultant homogeneous dispersion of the nanoparticles. However, this process suffers from the drawback of remaining the metal salts or complexes in the polymeric substrates, which gives rise to serious degradation of the polymeric matrix during curing (11, 12). Thus, some metal salts with strong acids groups could not be used as the metal oxide precursors and only certain metal complexes containing moderate organic acid groups could be added into the PI matrix at lower concentration levels. For instance, Taylor's group prepared PI/Fe_2O_3 composite films by the in situ synthesis approach through incorporation of iron(III) acetylacetonate, $Fe(acac)_3$ in poly(amic acid) (PAA) solution. The films were found very brittle during thermal treatment when the concentration of iron ions was more than 4 wt % (11).

Recently, several groups, including ours, reported that the surface metallized PI films could be prepared through the ion-exchange self-metallization technique (3, 4, 13, 14). This method mainly relies on chemical surface modification of PI films to form cation exchangeable groups (i.e., carboxyl groups) and subsequent incorporation of metal ions via ion-exchange reaction. Subsequent thermal treatment of the metal ion-loaded PI films induces metal ions reduction to give the metal surfaces without the addition of external reducing agent. In this article, we report on extending the

* Corresponding author. E-mail: wuzp@mail.buct.edu.cn (Z.P.W.). Tel: +86-10-64421693. Fax: +86-10-64421693.

Received for review September 13, 2009 and accepted November 12, 2009

DOI: 10.1021/am900620u

Scheme 1. Schematic Diagram of the Proposed Process for the Formation of Continuous NiO Layer on PI Substrate via Ion Exchange Technique

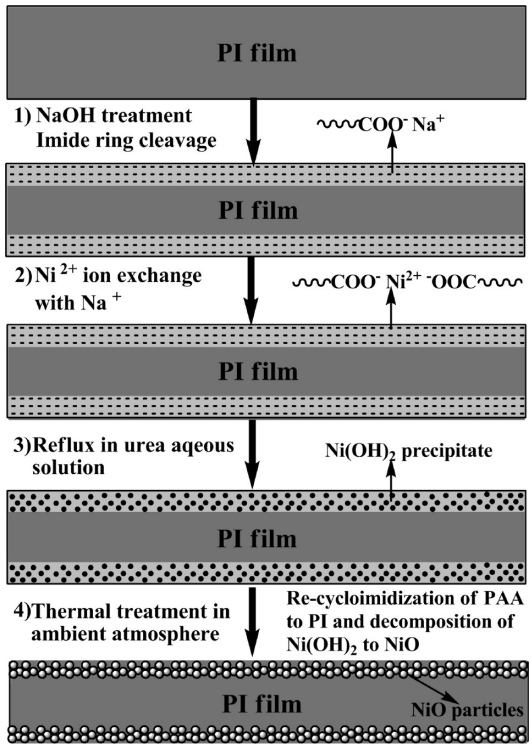

ion exchange technique to the fabrication of metal oxide layers strongly adhered to a flexible PI substrate. We selected NiO as a model metal oxide, because as one of the versatile and technologically important p-type semiconductors, it is widely used as catalysis (15), magnetic material (16), the p-type transparent conducting films (17), anode material for electrochromic devices (18), functional sensor layer for chemical sensor (19), the p-type layer for UV detector (20), and smart windows (19). The procedure for preparing PI/NiO nanocomposite films is shown in Scheme 1. Nickel ions were incorporated into the alkali-treated surface layers of PI films via an ion exchange process in nickel salt solution. Subsequent deposition process in urea solution made nickel ions convert to NiO precursor which decomposed to NiO nanoparticles during final thermal treatment in ambient air, resulting in a thin PI layer containing NiO nanoparticles. In this method, most common water-soluble nickel salts containing strong acid radicals, such as sulfate, hydrochloride, and nitrate, can be used as NiO precursors. During ion exchange in nickel salt solution, only positive ions are exchanged into the polymeric matrix, with no risk of strong acid radical being incorporated into the films (3). Besides, the nanocomposite film could maintain the excellent mechanical properties of original PI film for its inside is intact during the whole procedure. The most important is that microstructures such as the thickness of the composite layer and particle size could be controlled by initial alkali treatment conditions (time, concentration, and temperature), deposition conditions in urea solution (time, concentration, and temperature) and final annealing temperature (3, 13), respectively. In this paper, the effect of alkali treatment time on the morphologies and properties of the PI/NiO composite films was investigated and the formation mechanism of surface continuous NiO nanocomposite layer was proposed. We expect that the ion exchange technique could be extended to the fabrication of many metal oxides layers onto flexible PI surfaces for different potential applications.

EXPERIMENTAL SECTION

Materials. Pyromellitic dianhydrides oxidianiline (PMDA-ODA) PI films with thickness of 50 μm from Liyang Huajing Electronic Material Co., Ltd., Jiangsu province (China) were cleaned in distilled water at room temperature for 10 min under ultrasonication prior to use. Nickel sulfate hexahydrate ($NiSO_4 \cdot 6H_2O$) (>98.5%) with analytical quality was obtained from Sinopharm Chemical Reagent Co., Ltd. and used without further purification. Sodium hydroxide (NaOH) and urea ($CO(NH_2)_2$) with analytical quality were purchased from Beijing Chemicals Factory and Beijing Chemicals Reagent Company, respectively, and used as received.

Preparation of PI/NiO Composite Films. PI films were hydrolyzed in 2.5 M aqueous NaOH solution for 5, 8, and 12 h, respectively, at room temperature, and followed by washing with copious amount of deionized water. The nickel ions were incorporated by immersing the surface modified PI films into 0.4 M aqueous $NiSO_4$ solution for 1 h at room temperature, followed by rinsing with deionized water. The PI films were then transferred to a flask with 1 M aqueous urea solution and refluxed at 100 °C for 3 h. After being rinsed with deionized water and dried in ambient air, the films were thermally cured under tension in a forced oven. The cure cycles are heating over 3 h to 350 °C and then holding 3 h.

Characterization. X-ray photoelectron spectroscopy (XPS) investigations were carried out on an ESCALAB 250 spectrometer (Thermo Electron Corporation) using a monochromatic Al Kα X-ray source in the fixed analyzer transmission mode. The spectra were collected at a takeoff angle of 45°. The base pressure of the vacuum chamber was maintained at no more than 2×10^{-10} mbar during each measurement. Spectra presented in this study were calibrated by referencing the C 1s photopeak arising from aromatic PI backbone at binding energy (BE) of 284.6 eV and Shirley (nonlinear) background were subtracted. Full-width-at-half-maximum was kept the same for chemical components within the same core level of an element. In addition, all component peaks were set to be Gaussian-type.

X-ray diffractions (XRD) of the hybrid films were performed using an X-ray diffractometer (D/Max2500 VB2+/PC, Rigaku, Japan). The X-ray beam was generated by a Cu Kα target (λ = 0.154056 nm), using a tube voltage of 40 kV and a current of 200 mA. Scanning was conducted over the range of 2θ = 5−90° with a scanning rate of 0.17°/s.

The surface morphologies of the composite films were characterized with a scanning electron microscopy (SEM) (SEM-4700, Hitachi, Japan) at an accelerating voltage of 20 kV after samples were coated with ca. 5 nm of palladium−gold alloy. Transmission electron microscopy (TEM) was performed by employing an H-800 type Hitachi transmission electron microscope with an accelerate voltage of 200 kV. The samples for TEM were sectioned with an ultramicrotome with a diamond knife and then moved onto TEM copper grids for analysis.

Thermogravimetric analyses (TGA) and differential scanning calorimetry (DSC) were performed using a NETZSCH STAR 449C at a heating rate of 10 °C/min under an air atmosphere.

RESULTS AND DISCUSSION

PI/NiO Nanocomposites Preparation. The possible and ideal chemistry for the formation of PI/NiO composite films

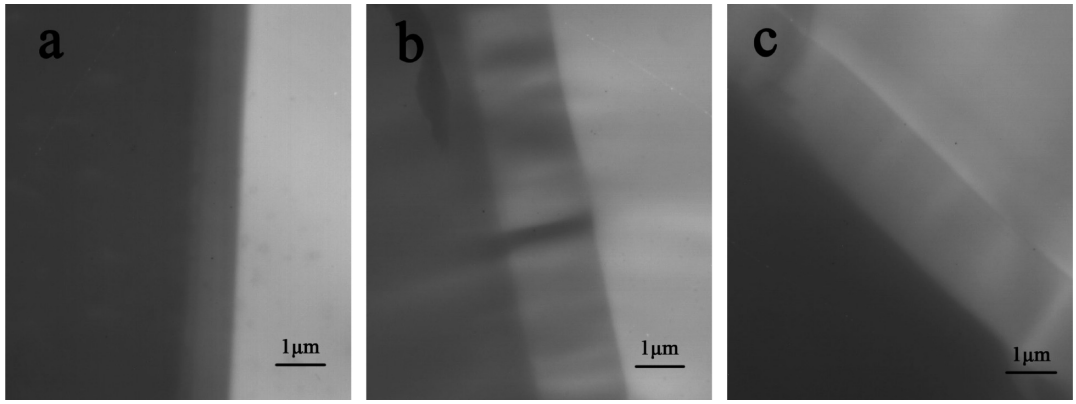

FIGURE 1. Cross-sectional TEM images for the PI films after 2.5 M NaOH treatment at room temperature for (a) 5, (b) 8, and (c) 12 h, respectively.

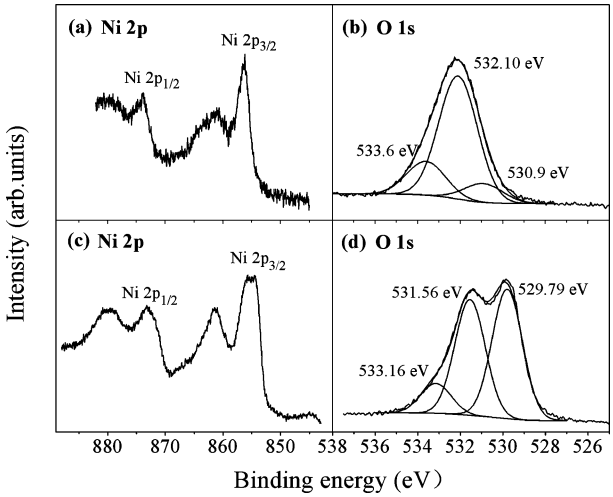

FIGURE 2. XPS measurement for the Ni 2p and O 1s core levels for the Ni^{2+}-loaded PI composite film: (a, b) after 1 M urea treatment at 100 °C for 3 h; (c, d) after 1 M urea treatment at 100 °C for 3 h and then thermal treatment at 350 °C for 3 h. The initial treatment time in 2.5 M NaOH solution is 12 h.

have been shown in Scheme 1. According to our previous report, sodium-polycarboxylate salt (sodium polyamate) would be formed in situ when PI films were immersed into the aqueous NaOH solution because of the hydrolytic cleavage of the imide groups contained in the repeating unit. The alkali treatment-promoted reaction allows precise control of the modified thickness of the PI film and the amount of the absorbed metal ions (3, 14). To fabricate continuous NiO layers, it is important to ensure enough nickel ions loading, which mainly depends on the modified thickness of PI films. As can be observed from the light color region in the SEM photos (Figure 1), after being treated in 2.5 M aqueous NaOH solution for 5, 8, and 12 h, the depth of the modified layer of PI films is 1, 1.8, and 2 μm, respectively, which suggests that the thickness of modified layers of PI substrate increases with increasing the alkali treatment time. However, further prolonging the alkali treatment time is not recommended because of the alkali etching effect (21). According to our observation, 12 h alkali treatment time, which corresponds to a modified thickness of about 2 μm, has been able to meet the demand for fabricating continuous NiO layer on PI substrate for the current commercial PI films.

During hydrothermal treatment of the nickel polyamate in aqueous urea solution, the absorbed nickel ions are converted to NiO precursors. Acting as a homogeneous precipitant, urea gradually decomposes to CO_2 and NH_3 at temperatures above 75−100 °C. Protolysis reaction of the ammonia slowly releases hydroxyl. The hydroxyl combines with the absorbed Ni^{2+} in the surface-modified layer of PI film to form $Ni(OH)_2$ precipitant. In final thermal treatment process in ambient air, the polyamate recycloimidizes to PI and the $Ni(OH)_2$ precipitates decompose to NiO nanoparticles. The conversion of PAA to PI during thermal treatment was confirmed by IR absorption spectroscopy in our previous report (4). The possible chemical reactions in urea solution and in thermal treatment process are listed below. The formation of $Ni(OH)_2$ after urea treatment and NiO after thermal treatment will be demonstrated by XPS observation (or measurement).

$$NH_2CONH_2 + 3H_2O \rightarrow CO_2 + 2NH_3 \cdot H_2O \quad (1)$$

$$NH_3 \cdot H_2O \rightarrow NH_4^+ + OH^- \quad (2)$$

$$-COO^-Ni^{2+-}OOC- + 2NH_4^+ + 2OH^- \rightarrow 2NH_4^{+-}OOC- + Ni(OH)_2 \quad (3)$$

$$Ni(OH)_2 \rightarrow NiO + H_2O \quad (4)$$

XPS and XRD Characterization. Figure 2 displays the XPS spectra of nickel ion-doped PI film after urea treatment at 100 °C for 3 h (panels a and b in Figure 2) and followed thermal treatment in ambient air at 350 °C for 3 h (panels c and d in Figure 2), respectively. Figure 2a shows the main Ni $2p_{3/2}$ peak at 855.6 eV associated with a broad satellite at 862.1 eV, suggesting the formation of $Ni(OH)_2$ (22−24) on PI film surface after urea treatment. The formation of $Ni(OH)_2$ can also be confirmed by O 1s spectrum in Figure 2b. The curve fit of the O 1s spectrum is represented by three bands. The bands at 533.60 and 532.10 eV are attributed to the ether and amide functionalities of the PAA (11, 25), respectively. The peak at 530.9 eV corresponds to the hydroxyl in $Ni(OH)_2$ (22, 23). After thermal treatment of the $Ni(OH)_2$-deposited PI film at 350 °C for 3 h, the main Ni $2p_{3/2}$ X-ray photoelectron (XP) peak of the composite film

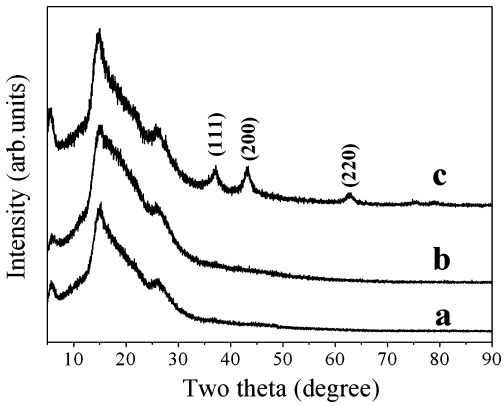

FIGURE 3. XRD patterns of (a) pristine PI film, the Ni^{2+}-loaded PI nanocomposite films after (b) urea treatment and (c) followed thermal treatment at 350 °C/3 h. The initial treatment time in 2.5 M NaOH solution is 12 h.

exhibits a double peak structure at about 854.83 eV with the Ni(Π) shakeup peak at 861.38 eV as shown in Figure 2c, which is consistent with BE measurement for NiO in literature (24, 26, 27). In Figure 2d, the O 1s XP peak shows three components at 529.79, 531.56, and 533.16 eV; the two contributions at high BE are corresponded to the imide and ether functionalities in PI, respectively (11, 25), whereas the component at 529.79 eV reveals the presence of Ni−O bands due to NiO particles. Thus from BE measurements for O 1s and Ni 2p core levels, it is clear that NiO particles formed on the surface of PI film. The XPS results suggest that the above proposed reactions (reaction 1−4) in urea treatment and final thermal treatment process are reasonable.

The formation of NiO particles on the PI surface layers can also be conformed through XRD analysis. Figure 3 shows the XRD patterns of pristine PI film, the $Ni(OH)_2$-deposited and then followed annealed PI composite films which were initially treated by 2.5 M NaOH solution for 12 h. In Figure 3a, the two broad peaks at 14.9 and 26° originated from the pristine aromatic PI with relatively low crystallinity. No other new diffraction peaks appear in Figure 3b. After 3 h thermal treatment at 350 °C, three diffraction peaks emerge at 37.16, 43.02, and 62.58°, as shown in Figure 3c. These three diffraction peaks can be perfectly indexed as (111), (200), and (220) crystal planes of the cubic structure crystalline NiO, which is consistent with that of the reported value (JCPDS Card no. 47−1049), and no obvious reflection peaks assignable to other impurities can be detected. The XRD result shows that NiO particles formed on the surface layers of PI film after thermal treatment. The result coincides well with the XPS results in Figure 2. In terms of the Debye−Scherrer equation, the average crystal size of NiO nanoparticles is 12.62 nm.

SEM and TEM Characterization. Figure 4a and 4b display the SEM images of the PI films after treatment in 2.5 M NaOH solution for 12 h and followed hydrothermal treatment in urea solution at 100 °C for 3 h without nickel ion-doping. The alkali-treated PI film presents a rough surface which is in favor of ion-exchange, as shown in Figure 4a. After direct hydrothermal treatment of the alkali-treated PI film in urea solution, the PI film surfaces become much rougher because of the continuing hydrolysis effect. Initially, the aqueous urea solution is a neutral environment, and then slowly turns to weak alkaline with increasing hydroxyl, owing to hydrolysis of urea at about 100 °C. The surface modified layers of PI films would be further hydrolyzed in the weak alkaline solution at about 100 °C, causing much rougher surfaces. As mentioned above, due to the alkali etching effect during the whole alkali treatment process, the hydrothermal treatment time in urea solution should also be controlled. Figure 4c−f show the SEM images of the nickel ion-doped PI films after treatment in aqueous urea solution for 2−5 h. With increasing treatment time in urea solution, the film surfaces become much rougher. Many big holes appear on the PI film surface when the treatment time in aqueous urea solution is longer than 3 h. Besides, the surfaces of the $Ni(OH)_2$-deposited PI films obtained at different urea treatment time are rougher than that of the PI film after alkali treatment, indicating that the surface etching effect of the PI film in urea solution are much serious than that in aqueous NaOH solution. To ensure enough nickel ions in the modified layer covert to $Ni(OH)_2$, in the meantime, to avoid serious etching effect, 3 h hydrothermal treatment in urea solution is appropriate for fabricating the $Ni(OH)_2$-deposited PI films. Although the film micromophology changed dramatically upon urea treatment time, there was no appreciable difference in appearance between the $Ni(OH)_2$-deposited PI films and the nickel ion-doped PI film. The $Ni(OH)_2$-deposited PI films were transparent and kept the same light yellow color with that of the pristine PI film. Figure 5a−c shows the SEM images for the $Ni(OH)_2$-deposited PI films with different initial treatment time in aqueous NaOH solution. It can be observed that increasing surface modification time in alkali solution results in much rougher surfaces of PI films after urea treatment. The $Ni(OH)_2$-deposited PI films initially treated in alkali solution for 8 and 12 h have similar surface morphology, which may be due to the significant etching of the films with similar thickness of alkali-treated layer during urea treatment. Table 1 lists the surface atomic concentration of the nickel ion-doped PI film after urea treatment and then thermal treatment derived from XPS measurement. The surface Ni atom concentration of the nickel ion-doped PI film after urea treatment is only about 1.27%, suggesting very few $Ni(OH)_2$ particles on the outmost surface of PI film. Therefore, it is hard to distinguish $Ni(OH)_2$ nanoparticles from the rough surfaces of PI films in Figure 4 as most of the $Ni(OH)_2$ nanoparticles with very small size are homogenously dispersed in the bulk of the alkali treated layers. After thermal treatment at 350 °C for 3 h of the $Ni(OH)_2$-deposited PI film, the surface Ni atom concentration of the final nanocomposite shifts up to 20.75%, indicating the aggregation of NiO clusters on the PI film surface. Figure 6 are the SEM images of the PI/NiO composite films obtained at 350 °C/3 h. NiO particles with about an average 10 nm size are homogenously dispersed on the surface of PI film that initially treated in alkali solution for

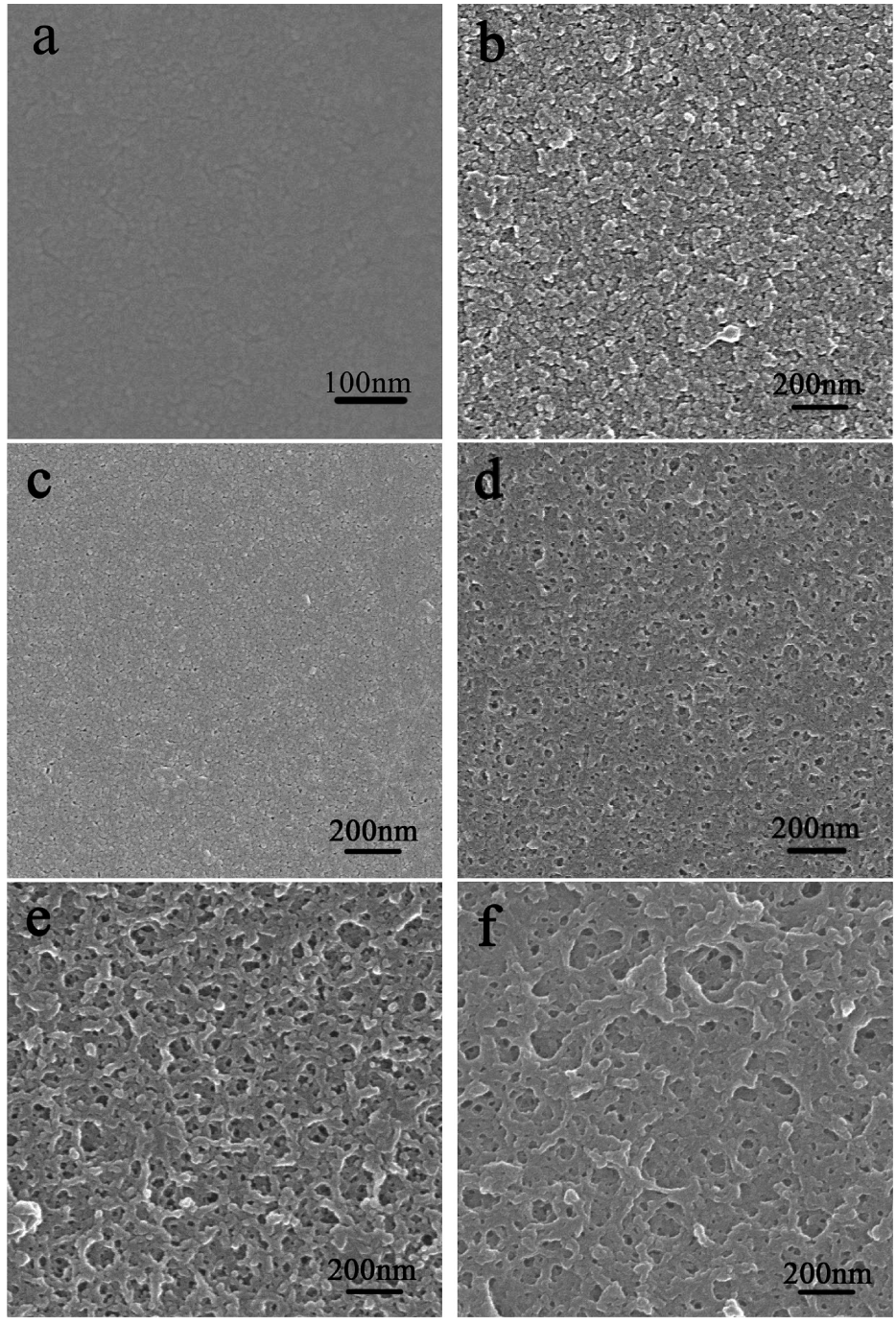

FIGURE 4. SEM images for the PI films (a) after NaOH treatment for 12 h, (b) followed treated by 1 M urea solution at 100 °C for 3 h without nickel ion loading, and the Ni^{2+}-absorbed PI films after 1 M urea treatment at 100 °C for (c) 2,(d) 3, (e) 4, and (f) 5 h, respectively.

5 h. For the films initially treated in alkali solution for 8 and 12 h, NiO particles with average size of about 10−15 nm are closely packed on the surface of the PI films. Though NiO nanoparticles contact with each other and form continuous layer, XPS surface composition data (Table 1) shows that carbon, nitrogen, and oxygen are abundant. This indicates that the NiO nanoparticles are embedded in PI matrix surface layer or the NiO nanoparticles and PI matrix are intermixed.

Figure 7 shows the cross-sectional TEM images of the $Ni(OH)_2$ deposited PI film and PI/NiO nanocomposite film that were initially treated by 2.5 M NaOH solution for 12 h. Compared with the light color region of the modified surfaces (Figure 1c), the darker region surface in Figure 7a suggests that $Ni(OH)_2$ nanoparticles homogenously disperse in the modified polymeric matrix. That is, $Ni(OH)_2$ clusters form in the bulk of the modified layers. Figure 7b shows that NiO particles are uniformly dispersed on PI surface and the NiO-embedded layer is much thinner than the NaOH-modified layer and $Ni(OH)_2$-deposited layer. The thickness decrease of the NiO composite layers during thermal treatment is probably caused by decomposition of PI matrix catalyzed by the newly born NiO nanoparticles. We will discuss it in detail below.

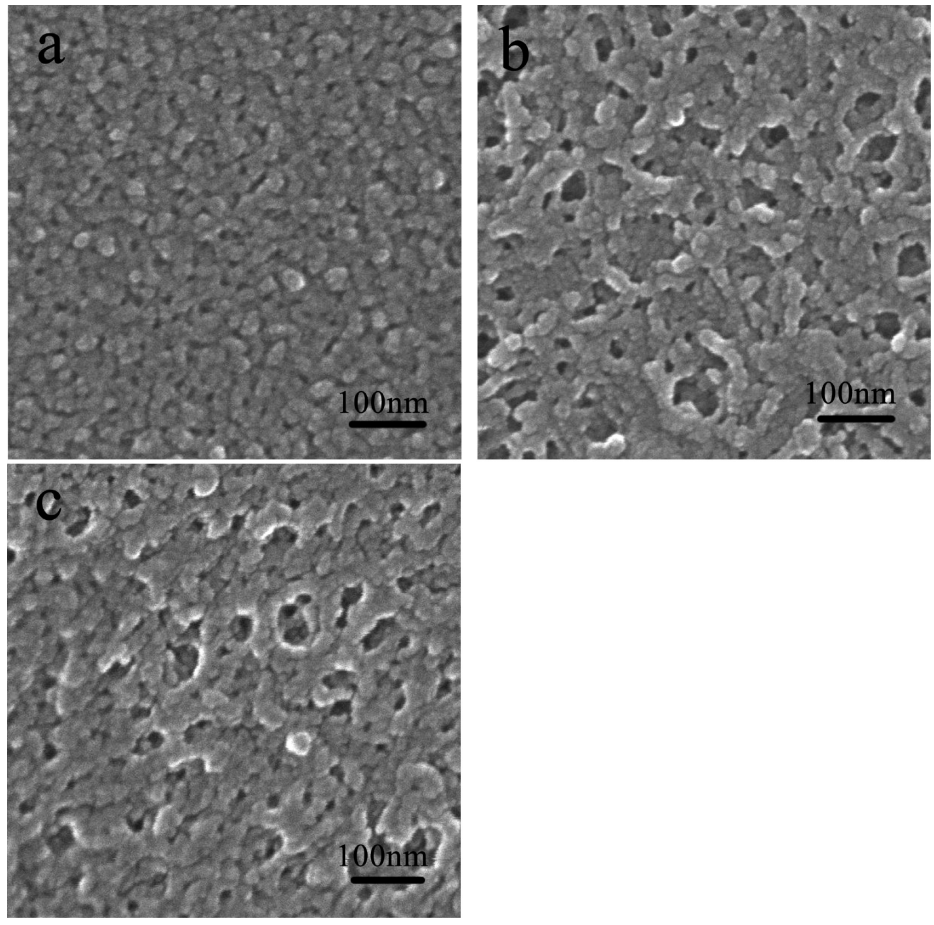

FIGURE 5. SEM images for the Ni^{2+}-absorbed PI films after 1 M urea treatment at 100 °C for 3 h, initial NaOH treatment time: (a) 5, (b) 8, and (c) 12 h, respectively.

Table 1. Surface Atomic Concentration for the Ni^{2+}-Absorbed PI Composite Films after 1 M Urea Treatment at 100 °C for 3 h and Then Thermal Treatment at 350 °C for 3 h (NaOH Treatment Time = 12 h)

	atomic concentrations (%)			
sample	Ni(2p)	C(1s)	O(1s)	N(1s)
after urea treatment	1.33	71.40	22.21	5.06
after thermal treatment at 350 °C/3 h	20.75	35.94	41.74	1.58

TG-DSC Analysis. To further understand the aggregation of NiO particles and the formation of surface-continuous NiO nanocomposite layer more clearly, we conducted TG and DSC characterizations of the $Ni(OH)_2$-deposited PI film. Figure 8 illustrates the TG-DSC profiles of the $Ni(OH)_2$-deposited PI composite film from the room temperature to 700 °C in air. The PI composite film underwent multistep weigh loss. The initial weight loss of about 8% at 90−120 °C represents the removal of the physically adsorbed water molecules. The followed main weight loss of about 20% occurs between 250 and 420 °C, and a broad and strong exothermic peak appears at the same temperature range in the DSC curve. We suggest that the weight loss in this temperature range is caused by the dehydration of $Ni(OH)_2$ to form NiO and the oxidative degradation of PI film catalyzed by the newly born NiO nanoparticles. $Ni(OH)_2$ undergoes decomposition reaction to form NiO at about 298−342 °C (28). Because of the nanosize effect, the newly born NiO particles have strong catalytic effect and they will catalyze the oxidative degradation of the surrounding PI below the oxidative decomposition temperature of pristine PI, during which NiO nanoparticles come to aggregate with each other to form continuous NiO layers. The sharp increase of surface nickel atom concentration after thermal treatment in Table 1 indicates the aggregation of NiO clusters on PI film surfaces. Therefore, the strong exothermic peak between 280 and 420 °C is probably corresponded to the oxidative degradation of PI catalyzed by the newly generated small NiO nanoparticles. The metal oxide-catalyzed oxidative decomposition of PI has been observed in other PI nanocomposites containing transional metal oxides such as cobalt oxide (8), iron oxide (11, 12), and titania (29). Once the smaller NiO nanoparticles aggregate together, their catalysis effect decreases rapidly as no obvious weight loss is observed above 430 °C. Until 500 °C, another main weight loss of about 63% appears in the TG curves with a narrow and strong exothermic peak at 588 °C in DSC curve, corresponding to the thermal oxidative degradation of PI matrix. Figure 9 depicts the TG and DSC curves of the pristine PI film and PI/NiO composite films. For the pristine PI film, there is only one obvious weight loss in TG curve

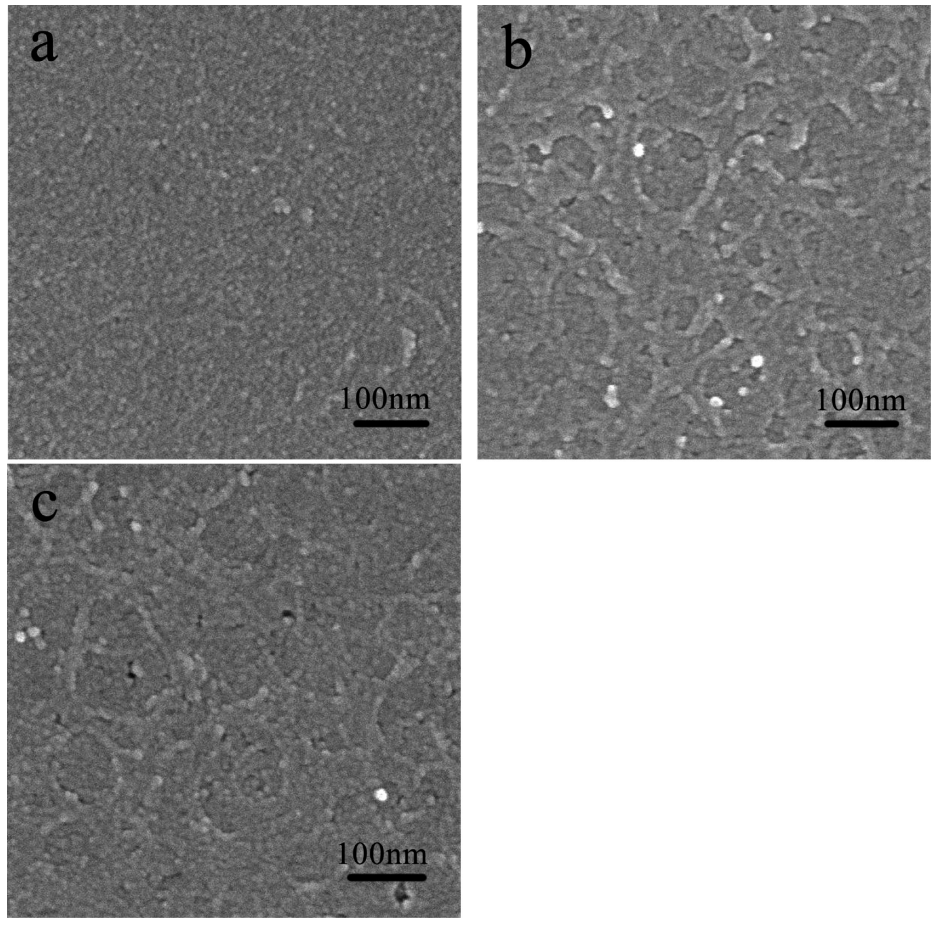

FIGURE 6. SEM images of the PI/NiO nanocomposite films obtained at 350 °C/3 h, initial NaOH treatment time: (a) 5, (b) 8, and (c) 12 h.

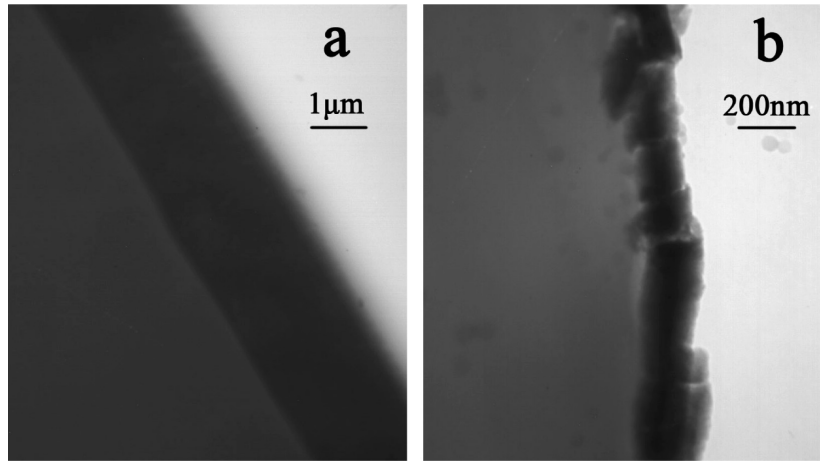

FIGURE 7. TEM images of (a) the Ni^{2+}-doped PI films after 1 M urea treatment at 100 °C for 3 h and (b) the PI/NiO nanocomposite films obtained at 350 °C/3 h. The initial treatment time in 2.5 M NaOH solution is 12 h.

with a strong exothermic peak at 588 °C in DSC curve, corresponding to the oxidative decomposition of PI. For the PI/NiO composite films, there is also only one main weight loss in the same temperature range. This reveals that the formed surface continuous NiO layer has little effect on the thermal stability of the PI films. By comparing the TG-DSC curves of the pristine PI film, the $Ni(OH)_2$ deposited PI film and PI/NiO nanocomposite films, it seems that the decomposition of surrounding PI matrix catalyzed by the newly generated small NiO particles during thermal treatment contributes much to the aggregation of surface NiO nanoparticles and the formation of a continuous NiO nanocomposite layer.

CONCLUSION

PI composite films with NiO nanocomposite layers embedded on their both surfaces were successfully prepared by thermal calcination of the precursor films that were obtained by chemical deposition of the nickel ion-absorbed PI films in aqueous urea solution. Continuous NiO nanocom-

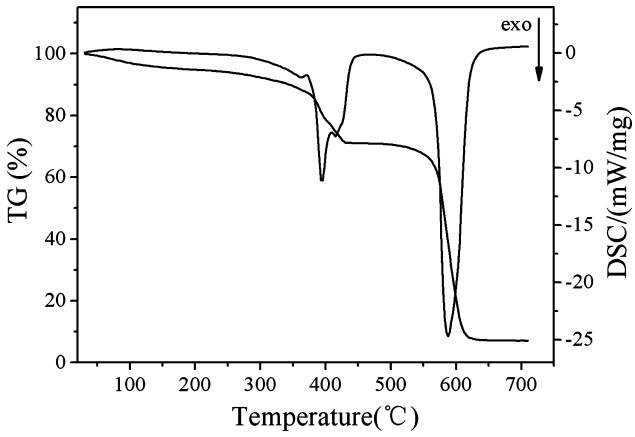

FIGURE 8. TG-DSC curves of the Ni^{2+}-absorbed PI film after 1 M urea treatment at 100 °C for 3 h. The initial treatment time in 2.5 M NaOH solution is 12 h.

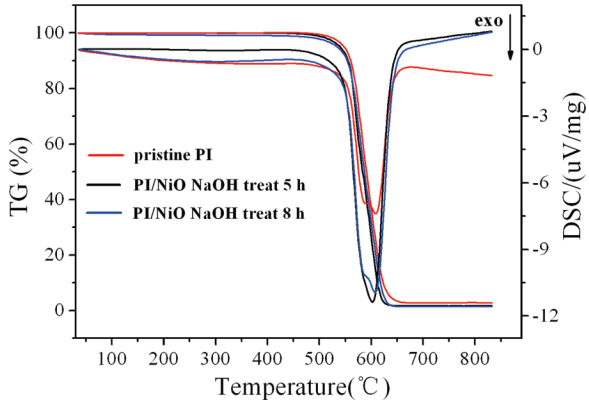

FIGURE 9. TG-DSC curves of the pristine PI film and the PI/NiO nanocomposite films obtained at 350 °C/3 h.

posite layers with NiO average diameter of 10−15 nm formed on both surfaces of the PI films by varying initial treatment time in alkali solution. XPS characterization indicated the precursor of the NiO after deposition in urea solution was $Ni(OH)_2$. SEM, TEM, and TG-DSC results showed that the formation of surface continuous NiO nanocomposite layers was accompanied by the oxidative decomposition of surrounding PI matrix catalyzed by the newly born NiO nanoparticles, during which the NiO particles come into contact with each other. The final PI/NiO composite films maintained the excellent thermal property of the pristine PI film. Such ion exchange technique provides a promising route for preparing morphology-controlled PI/metal oxide nanocomposites.

Acknowledgment. This research was financially supported by the program for the National High Technology Research and Development (Project No.2007AA03Z537) of China (863 Program), the National Natural Science Foundation of China (NSFC, Project 50973006), and the Program for Changjiang Scholars and Innovative Research Team in University (PCSIRT, IRT0706).

REFERENCES AND NOTES

(1) Qi, S. L.; Wu, Z. P.; Wu, D. Z.; Wang, W. C.; Jin, R. G. *Chem. Mater.* **2007**, *19*, 393–401.
(2) Qi, S. L.; Wu, Z. P.; Wu, D. Z.; Jin, R. G. *J. Phys. Chem. B* **2008**, *112*, 5575–5584.
(3) Wu, Z. P.; Wu, D. Z.; Yang, W. T.; Jin, R. G. *J. Mater. Chem.* **2006**, *16*, 310–316.
(4) Wu, Z. P.; Wu, D. Z.; Qi, S. L.; Zhang, T.; Jin, R. G. *Thin Solid Films* **2005**, *493*, 179–184.
(5) Vijayanand, H. V.; Arunkumar, L.; Gurubasawaraj, P. M.; Veeresha Sharma, P. M.; Basavaraja, S.; Saleem, A.; Venkataraman, A.; Ghanwat, A.; Maldar, N. N. *J. Appl. Polym. Sci.* **2007**, *103*, 834–840.
(6) Hsu, S. C.; Whang, W. T.; Hung, C. H.; Chiang, P. C.; Hsiao, Y. N. *Macromol. Chem. Phys.* **2005**, *206*, 291–298.
(7) Matsumura, M.; Camata, R. P. *Thin Solid Films* **2005**, *476*, 317–321.
(8) Rancourt, J. D.; Taylor, L. T. *Macromolecules* **1987**, *20*, 790–795.
(9) Rancourt, J. D.; Rorta, G. M.; Taylor, L. T. *Thin Solid Films* **1988**, *158*, 189–206.
(10) Nandi, M.; Conklin, J. A., Jr., L. S.; Sen, A. *Chem. Mater.* **1990**, *2*, 772–776.
(11) Bergmeister, J. J.; Rancourt, J. D.; Taylor, L. T. *Chem. Mater.* **1990**, *2*, 640–641.
(12) Bergmeister, J. J.; Rancourt, J. D.; Taylor, L. T. *Chem. Mater.* **1992**, *4*, 729–737.
(13) Ikeda, S.; Akamatsu, K.; Nawafune, H.; Nishino, T.; Deki, S. *J. Phys. Chem. B* **2004**, *108*, 15599–15607.
(14) Akamatsu, K.; Ikeda, S.; Nawafune, H.; Deki, S. *Chem. Mater.* **2003**, *15*, 2488–2491.
(15) Song, X. F.; Gao, L. *J. Phys. Chem. C* **2008**, *112*, 15299–15305.
(16) Seto, T.; Akinaga, H.; Takano, F.; Koga, K.; Orii, T.; Hirasawa, M. *J. Phys. Chem. B* **2005**, *109*, 13403–13405.
(17) Sasi, B.; Gopchandran, K. G.; Manoj, P. K.; Koshy, P.; Prabhakara, Rao. P.; Vaidyan, V. K. *Vacuum* **2002**, *68*, 149–154.
(18) Zhang, F. B.; Zhou, Y. K.; Li, H. L. *Mater. Chem. Phys.* **2004**, *83*, 260–264.
(19) Ferreira, F. F.; Tabacniks, M. H.; Fantini, M. C. A.; Faria, I. C.; Gorenstein, A. *Solid State Ionics* **1996**, *86−88*, 971–976.
(20) Choi, J. M.; Im, S. *Appl. Sur. Sci.* **2005**, *244*, 435–438.
(21) Huang, X. D.; Bhangale, S. M.; Moran, P. M.; Yakovlev, N. L.; Pan, J. S. *Polym. Int.* **2003**, *52*, 1064–1069.
(22) Lin, T. C.; Seshadri, G.; Kelber, J. A. *Langmuir* **1998**, *14*, 3673–3681.
(23) Park, K. W.; Choi, J. H.; Kwon, B. K.; Lee, S. A.; Sung, Y. E. *J. Phys. Chem. B* **2002**, *106*, 1869–1877.
(24) Davidson, A.; Tempere, J. F.; Che, M.; Roulet, H.; Dufour, G. *J. Phys. Chem.* **1996**, *100*, 4919–4929.
(25) Girardeaux, C.; Druet, E.; Demoncy, P.; Delamar, M. *J. Electron Spectrosc. Relat. Phenom.* **1994**, *70*, 11–21.
(26) Petitto, S. C.; Marsh, E. M.; Langell, M. A. *J. Phys. Chem. B* **2006**, *110*, 1309–1318.
(27) Arranz, A.; Palacio, C. *Langmuir* **2002**, *18*, 1695–1701.
(28) Liang, Z. H.; Zhu, Y. J.; Hu, X. L. *J. Phys. Chem. B* **2004**, *108*, 3488–3491.
(29) Chiang, P. C.; Whang, W. T. *Polymer* **2003**, *44*, 2249–2254.

AM900620U